8th International IFAC Symposium on
Dynamics and Control of Process Systems
Preprints Vol.1, June 6-8, 2007, Cancún, Mexico

ROBUST CONTROL OF A SOLIDIFICATION PROCESS WITH PARAMETRIC UNCERTAINTY

Beathe Furenes *, **Bernt Lie** *

* *Telemark University College, P.O. Box 203, N-3901 Porsgrunn, Norway*

Abstract: Robust control of a solidification process is considered. In solidification processes, the properties of the solidified material are significantly determined by the solidification rate, defined as the time derivative of the solid/liquid interface position. Most often the position can not be measured directly, and thus the interface position must be estimated in order to employ feedback control. The solidification model has a variable structure where the state equations depend on the interface position. An observer based on a linearized model is developed. A gain-scheduled PI-controller is implemented, and the robustness properties are tested for parametric uncertainty in the model.

Keywords: Robust control, state estimation, phase transition

1. INTRODUCTION

Robustness of a system refers to a system that functions adequately for all admissible uncertainties. Sources for system uncertainty may be poor plant knowledge, uncertain or slowly varying parameters, nonlinearities (e.g. hysteresis or friction), errors or unknown initial conditions, reduced-order models, additive unknown internal or external noise, and environmental influence (Weinmann, 1991).

In some systems, there are no measurements of the output to be controlled. Instead, other output variables are measured. Then, if the system is observable, the controlled output can be estimated from the other measured outputs. The separation principle states that for linear systems the state feedback control and an observer can be designed independently (Friedland, 1986). However, a critical assumption for the separation principle is that the observer includes an exact dynamic model of the plant, which is almost never valid in reality since the precise dynamic model is rarely known. Thus, it is of importance to check the robustness properties of the system when the controller and observer are designed through the use of the separation principle.

In solidification processes, the solidification rate significantly determines the properties of the solidified material. Some processes require certain solidification rates in order to achieve well-defined microstructures, and the solidification rate may also affect the capturing of impurities in the solid phase. By controlling the solidification rate, the product quality can often be improved.

In order to employ feedback control of the solidification rate, a measurement or reliable online estimate of the interface position must be available. An example of direct measurement of the interface position is given in Drevermann *et al.* (2004*b*). The movement of the interface is measured by an ultrasonic pulse-echo technique which can be used for rod-like sample geometries

(Drevermann *et al.*, 2004*a*), and thus estimation of the interface position is not necessary. However, in most industrial casting processes, the interface position can not be measured directly. In most cases, the only data available are temperatures at the mould walls or in the melt, and hence the interface position must be estimated from the measured temperatures.

Methods for designing and analyzing robustness properties in control and estimation systems are described e.g. in the books Burl (1999), Skogestad and Postlethwaite (1996) and Petersen and Savkin (1999). Previous work on state estimation and feedback control for casting operations are reported in Ray *et al.* (1979), Greiss and Ray (1980), and Batur *et al.* (1999). However, robustness issues are not treated in these works.

In this paper, a simple one-dimensional solidification model based on first principles is used to estimate the interface position and the temperature dynamics for a pure substance. The model is linearized numerically, and a Kalman filter is implemented based on the linearized model at different operating points. A gain-scehduled PI-controller is implemented in order to control the solidification rate. Robust stability is tested on the closed-loop system for parametric uncertainty in the model.

The paper is organized as follows: In the second section the general control configuration is described together with conditions for robustness properties. Then the solidification model is described and some assumptions are given. In the subsequent section the model is linearized numerically. Next, the Kalman filter gain is calculated, and then some simulation results are presented. Finally, some conclusions are presented.

2. A GENERAL CONTROL CONFIGURATION WITH UNCERTAINTY

Many linear control problems including model uncertainty can be formulated using the block diagram in figure 1 (Skogestad and Postlethwaite, 1996). P is the generalized plant model, K is the controller, and the perturbation Δ, assumed to be bounded, represents the uncertainty. The control signal u is generated from the controller, K, based on information in the sensed outputs v (e.g. commands, measured plant outputs, measured disturbances, etc). The exogenous inputs w may be commands, disturbances, and noise. The exogenous outputs, z, are error signals to be minimized. u_Δ is the perturbation input (the output of the feedback perturbation Δ), whereas y_Δ is the perturbation output (the input to the feedback perturbation Δ).

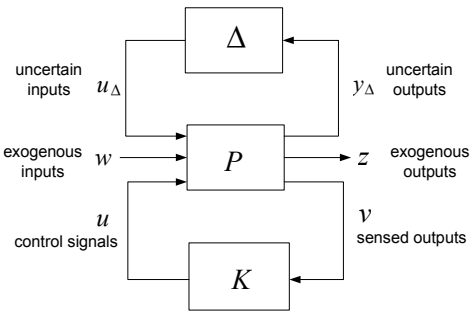

Fig. 1. General control configuration for the case with model uncertainty.

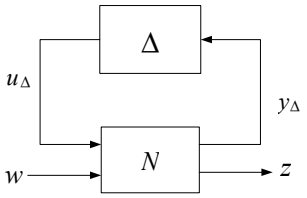

Fig. 2. $N\Delta$-structure for robust closed-loop performance analysis.

The plant P thus has three inputs and three outputs (each of which can be a vector), and can be written as

$$\begin{pmatrix} y_\Delta \\ z \\ v \end{pmatrix} = \begin{pmatrix} P_{y_\Delta u_\Delta} & P_{y_\Delta w} & P_{y_\Delta u} \\ P_{z u_\Delta} & P_{zw} & P_{zu} \\ P_{v u_\Delta} & P_{vw} & P_{vu} \end{pmatrix} \begin{pmatrix} u_\Delta \\ w \\ u \end{pmatrix} = P \begin{pmatrix} u_\Delta \\ w \\ u \end{pmatrix}. \quad (1)$$

In order to analyse stability and performance conditions for the uncertain closed-loop system, it is desirable to represent the uncertain system in the standard form given in figure 2. The nominal closed-loop transfer function $N(s)$ is found by closing the feedback loop for the controller, $u = Kv$, thus

$$\begin{pmatrix} y_\Delta \\ z \end{pmatrix} = \begin{pmatrix} N_{y_\Delta u_\Delta} & N_{y_\Delta w} \\ N_{z u_\Delta} & N_{zw} \end{pmatrix} \begin{pmatrix} u_\Delta \\ w \end{pmatrix} = N \begin{pmatrix} u_\Delta \\ w \end{pmatrix}, \quad (2)$$

where

$$\begin{aligned} N_{y_\Delta u_\Delta} &= P_{y_\Delta u_\Delta} + P_{y_\Delta u} \left(I - K P_{vu}\right)^{-1} K P_{v u_\Delta} \\ N_{y_\Delta w} &= P_{y_\Delta w} + P_{y_\Delta u} \left(I - K P_{vu}\right)^{-1} K P_{vw} \\ N_{z u_\Delta} &= P_{z u_\Delta} + P_{zu} \left(I - K P_{vu}\right)^{-1} K P_{v u_\Delta} \\ N_{zw} &= P_{zw} + P_{zu} \left(I - K P_{vu}\right)^{-1} K P_{vw}. \end{aligned}$$

It can be shown (Skogestad and Postlethwaite, 1996) that when N is nominally stable and when Δ is bounded, the stability of the system in figure 2 is equivalent to the stability of the $M\Delta$-structure in figure 3 where $M = N_{y_\Delta u_\Delta}$.

In the next subsections, conditions for checking the stability of the $M\Delta$-structure will be derived for unstructured and structured Δ.

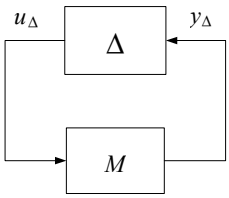

Fig. 3. $M\Delta$-structure for robust closed-loop stability analysis. $M = N_{y_\Delta u_\Delta}$ is the transfer function from u_Δ to y_Δ.

2.1 Robust stability for unstructured uncertainty

Unstructured uncertainty is often referred to as full-block complex perturbation uncertainty. Δ is then allowed to be any (full) complex transfer function matrix satisfying $\|\Delta\|_\infty \leq 1$.

If $M(s)$ is nominally stable and the perturbations $\Delta(s)$ are stable, then the $M\Delta$-structure in figure 3 is stable for all perturbations Δ satisfying $\|\Delta\|_\infty \leq 1$ if and only if (Skogestad and Postlethwaite, 1996)

$$\bar{\sigma}\left[M(j\omega)\right] < 1, \quad \forall\omega \Leftrightarrow \|M\|_\infty < 1. \tag{3}$$

2.2 Robust stability for structured uncertainty

If the uncertainty in the model is structured, i.e. Δ is block-diagonal, the above stability condition (3) is often too conservative. It is then desirable to obtain a tighter robust stability condition. The structured singular value $\mu(M)$ depends on both M and Δ, and thus takes advantage of the structure in the uncertainty. $\mu(M)$ is defined as (Skogestad and Postlethwaite, 1996)

$$\mu(M)^{-1} \triangleq \min_{\Delta} \left\{\bar{\sigma}\left(\Delta\right) | \det\left(I - M\Delta\right) = 0\right\}. \tag{4}$$

A general feedback system is internally stable for all possible block-diagonal perturbations with $\bar{\sigma}\left[\Delta(j\omega)\right] < 1, \forall\omega$, if and only if the nominal closed-loop system is internally stable and

$$\mu\left[M(j\omega)\right] \leq 1, \quad \forall\omega. \tag{5}$$

3. SYSTEM DEFINITION

The solidification process studied in this paper is sketched in figure 4. A mould with height L, assumed to be be covered by a thick layer of insulation on the vertical surfaces, is situated in a solidification chamber and is initially filled with melt. Heat is extracted from the melt by cooling the bottom mould wall at a rate $\dot{Q}_0$. At the top of the mould, the melt is heated at a rate $\dot{Q}_L$ by imposing electrical current on a resistance heater. As the solid begins to form, the interface position, h, and the temperature profiles $T_s(t,z)$ and $T_\ell(t,z)$, will change with time; subscripts s and ℓ refer to solid and liquid phase,

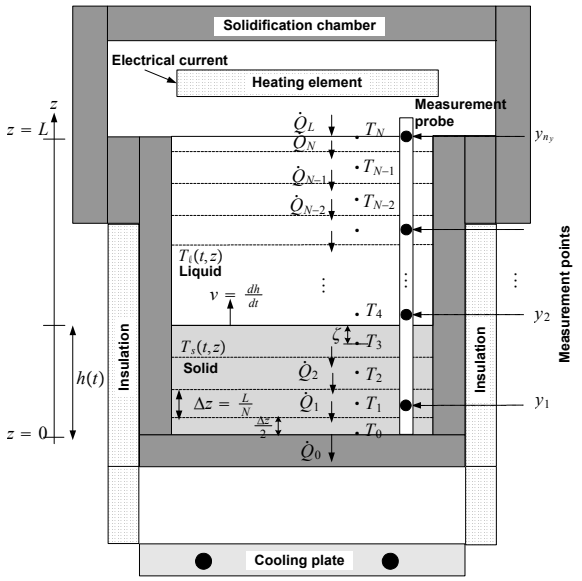

Fig. 4. Simplified sketch of the solidification process with available temperature measurements in the crucible.

respectively. For simplicity $\dot{Q}_0$ is assumed to be constant during solidification, whereas $\dot{Q}_L$ is used to control the solidification rate. The number of available (temperature) measurements in the melt are n_y, and the estimate of the interface position is based on the measured temperatures.

The mathematical model of this process is based on the heat diffusion equation. There is one fixed boundary condition and one moving boundary condition for both phases. The independent variables are time t and position z, and the resulting model is a system of two PDEs and one ODE. The spatial domain is split into two subdomains by the interface, one for each phase.

The discretization method is based on a fixed-grid finite-difference method, and is mainly taken from Chun and Park (2000). Details about the implementation of the model are found in Furenes and Lie (2006*a*).

The state vector with dimension $n_x = N + 1$ is given as

$$\mathbf{x} = \begin{pmatrix} x_1 & \cdots & x_N & x_{N+1} \end{pmatrix}^T = \begin{pmatrix} T_1 & \cdots & T_N & h \end{pmatrix}^T$$

where $T_1, ..., T_N$ are the temperatures in the spatial grid cells and N is the number of grid cells. h is the interface position. The input variables are

$$\mathbf{u} = \begin{pmatrix} u_1 & u_2 \end{pmatrix}^T = \begin{pmatrix} \dot{Q}_0 & \dot{Q}_L \end{pmatrix}^T$$

where, for simplicity, $\dot{Q}_0$ is assumed to be constant. Temperature measurements are available at n_y positions in the melt

$$y_m = \begin{pmatrix} y_1 & \cdots & y_{n_y} \end{pmatrix}^T,$$

where $n_y \leq N$.

Table 1. State definitions for the solidification model.

State definitions for the temperatures	Node no.(n)
$\frac{dT_n}{dt} = \alpha_n \left[\frac{T_{n+1} - T_n}{(\Delta z)^2} - \frac{\dot{Q}_0}{Ak_n \Delta z} \right]$	1
$\frac{dT_n}{dt} = \alpha_n \frac{T_{n+1} - 2T_n + T_{n-1}}{(\Delta z)^2}$	$(2, i-1)$, $(i+1, N-1)$
$\frac{dT_n}{dt} = \alpha_n \frac{\frac{\tilde{k}_\ell}{\tilde{k}_s} T_{n+1} - 2T_n + T_{n-1} + T_m \left(1 - \frac{\tilde{k}_\ell}{\tilde{k}_s}\right)}{(\Delta z)^2} + \frac{\alpha_n}{\tilde{k}_s} \frac{(1-\zeta)\Delta \hat{H}_f}{\Delta z} \frac{dh}{dt}$	i
$\frac{dT_n}{dt} = \alpha_n \frac{T_{n+1} - 2T_n + \frac{\tilde{k}_s}{\tilde{k}_\ell} T_{n-1} + T_m \left(1 - \frac{\tilde{k}_s}{\tilde{k}_\ell}\right)}{(\Delta z)^2} + \frac{\alpha_n}{\tilde{k}_\ell} \frac{\zeta \Delta \hat{H}_f}{\Delta z} \frac{dh}{dt}$	$i+1$
$\frac{dT_n}{dt} = 2\alpha_n \left[\frac{\dot{Q}_L}{Ak_n \Delta z} - \frac{T_n - T_{n-1}}{(\Delta z)^2} \right]$	N
State definition for the interface position	
$\frac{dh}{dt} = \frac{\tilde{k}_s}{\Delta \hat{H}_f} \frac{T_m - [(1-\zeta) T_{i-1} + \zeta T_i]}{\Delta z} - \frac{\tilde{k}_\ell}{\Delta \hat{H}_f} \frac{[(1-\zeta) T_{i+1} + \zeta T_{i+2}] - T_m}{\Delta z}$	–

The controlled output is

$$y_c = h.$$

The definition of the state equations for the temperatures and the position vary with the nodal index i, where the interface position is located between node indices i and $i+1$. The model thus has a variable structure of the system of the form

$$\frac{dx_k}{dt} = f_k(\mathbf{x}, \mathbf{u}, i) \text{ for } k = 1, .., N+1\,,$$

where i can be found by comparing the nodal temperatures with the melting temperature, T_m:

$$i = \max_k (T_k \leq T_m)\,, \quad k = 1, .., N.$$

The state space model for the temperatures and the interface position are given in Table 1. The dimensionless distance from the interface position h to node i is given by

$$\zeta = \zeta(h) = \frac{h - i\Delta z}{\Delta z}.$$

The grid size is $\Delta z = L/N$ and $\tilde{k} = k/\rho$.

Figure 5 shows the scaled temperature distribution and the interface position as functions of time at constant heating and cooling conditions.

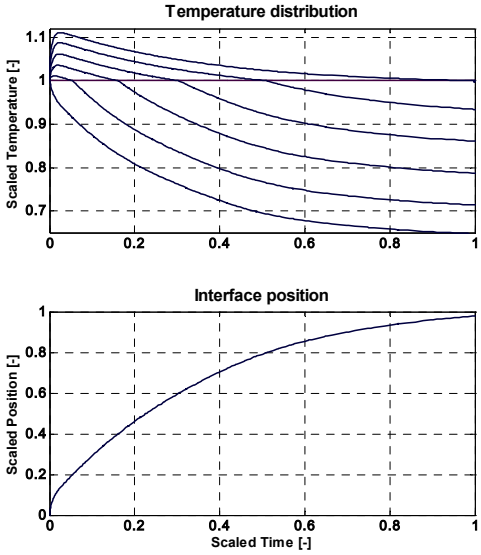

Fig. 5. Simulation of the solidification model with $N = 50$ discretization elements. Temperature distribution and interface position (all scaled) for constant cooling and heating conditions.

4. STATE ESTIMATION

4.1 Linearization of the model

Since the solidification process is a batch process, there exists no single operating point around which the system can be linearized (Bonvin, 1998). The solidification model undergoes structural changes in the definition of the state variables each time the interface position crosses a grid line (when the nodal index i changes), and hence the system is linearized around a trajectory given by the interface position. The A and B matrices will change with the nodal index i, and hence the A and B matrices need to be calculated for every index $i \in 1, ..., N$, whereas the C-matrix is independent of the index. The procedure of the switching between the different systems is handled by the events function, and is described in (Furenes and Lie, 2006*b*).

4.2 Calculation of steady state Kalman filter gains

The different A matrices were used as inputs to the steady state Kalman filter gain algorithm (see e.g. (Lewis, 1986) for more information on Kalman filter theory), and thus the Kalman gain K_f values also depends on the interface position. The switching between the different filter gains follows the model switching.

5. CONTROLLER DESIGN AND NOMINAL STABILITY

A gain-scheduled PI controller is used. The stability margins for 3 operating points are shown in Table 2, where $S = (I + L)^{-1}$, $T = (I + L)^{-1} L$, $L = GK_c$, and $G = E(sI - A)^{-1} B$. It should be noted that even though the linearized system is stable, this does not guarantee the overall nonlinear system to be stable.

Table 2. Stability margins and maximum peaks for the nominal system at 3 operating points. $M_T = \max_\omega |T(j\omega)|$ and $M_S = \max_\omega |S(j\omega)|$.

h	PM [°]	GM [dB]	M_S [dB]	M_T [dB]
0.5	37	17	3.8	1.1
0.7	56	18	3.5	0.6
0.9	65	58	2	0

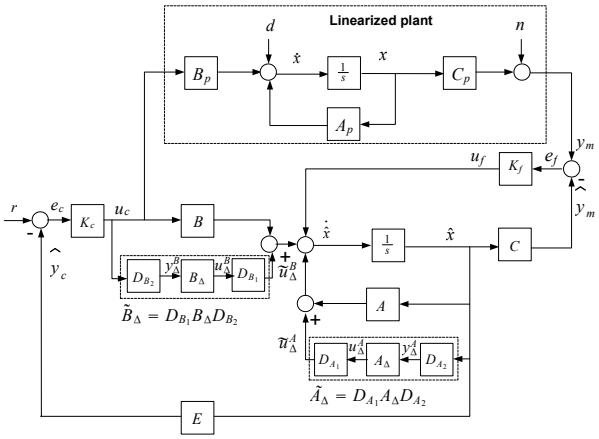

Fig. 6. Uncertain linearized process with Kalman filter and control feedback.

6. ROBUSTNESS TESTS

The uncertain linearized system for estimation and control of the interface position can be represented in state space form as shown in figure 6. K_f is the Kalman filter gain, K_c is the controller transfer function, $\tilde{A}_\Delta$ represents uncertainty in the A-matrix, and $\tilde{B}_\Delta$ represents uncertainty in the B-matrix. The measurement matrix is assumed to contain no uncertainty.

The signals for the generalized plant are identified in Table 3.

Table 3. Definition of the signals in the uncertain system.

Signal	Definition
Sensed outputs:	$v = \begin{pmatrix} e_c & e_f \end{pmatrix}^T = \begin{pmatrix} r - \hat{y}_c & y_m - \hat{y}_m \end{pmatrix}^T$
Control signals:	$u = \begin{pmatrix} u_c & u_f \end{pmatrix}^T$
Exogenous inputs:	$w = \begin{pmatrix} r & d & n \end{pmatrix}^T$
Exogenous outputs:	$z = \begin{pmatrix} e_c & e_f \end{pmatrix}^T$
Uncertain inputs:	$u_\Delta = \begin{pmatrix} u_\Delta^A & u_\Delta^B \end{pmatrix}^T$
Uncertain outputs:	$y_\Delta = \begin{pmatrix} y_\Delta^A & y_\Delta^B \end{pmatrix}^T$

6.1 Open loop system (obtaining P)

The estimated states are given by

$$\dot{\hat{x}} = A\hat{x} + \tilde{u}_\Delta^A + Bu_c + \tilde{u}_\Delta^B + u_f \quad (6)$$

$$\hat{y}_m = C\hat{x}. \quad (7)$$

where $A \in \mathbb{R}^{n_x \times n_x}$, $B \in \mathbb{R}^{n_x \times n_{u_c}}$, $C \in \mathbb{R}^{n_{y_m} \times n_x}$, and

$$\tilde{u}_\Delta^A = \tilde{A}_\Delta \hat{x},\ \tilde{u}_\Delta^B = \tilde{B}_\Delta u_c.$$

The perturbations $\tilde{A}_\Delta$ and $\tilde{B}_\Delta$ must be pulled out in Δ such that Δ has the structure

$$\Delta = \begin{pmatrix} A_\Delta & 0 \\ 0 & B_\Delta \end{pmatrix}, \quad (8)$$

and where

$$\|A_\Delta\|_\infty \le 1,\ \|B_\Delta\|_\infty \le 1 \quad (9)$$

for all possible perturbations $\tilde{A}_\Delta$ and $\tilde{B}_\Delta$. This can be done by factoring $\tilde{A}_\Delta$ and $\tilde{B}_\Delta$ into

$$\tilde{A}_\Delta = D_{A_1} A_\Delta D_{A_2},\ \tilde{B}_\Delta = D_{B_1} B_\Delta D_{B_2}$$

provided that equation (9) holds. $\tilde{A}_\Delta$ is decomposed by QR-factorization into

$$\tilde{A}_\Delta = QR = D_{A_1} D_{A_2} = D_{A_1} I_{n_x} D_{A_2} = D_{A_1} A_\Delta D_{A_2}.$$

The same procedure is performed on $\tilde{B}_\Delta$. Thus, $A_\Delta = B_\Delta = I_{n_x}$ for all possible perturbations $\tilde{A}_\Delta$ and $\tilde{B}_\Delta$, and equation (9) holds.

In order to derive the generalized plant, P, expressions for y_Δ and w as functions of u_Δ and u must be found. The elements of P needed in the calculation of $M = N_{y_\Delta u_\Delta}$ are

$$P_{y_\Delta u_\Delta} = \begin{pmatrix} D_{A_2} G_p D_{A_1} & D_{A_2} G_p D_{B_1} \\ 0 & 0 \end{pmatrix}$$

$$P_{y_\Delta u} = \begin{pmatrix} D_{A_2} G_p B_u & D_{A_2} G_p \\ D_{B_2} & 0 \end{pmatrix}$$

$$P_{v u_\Delta} = \begin{pmatrix} -E G_p D_{A_1} & -E G_p D_{B_1} \\ -C G_p D_{A_1} & -C G_p D_{B_1} \end{pmatrix}$$

$$P_{vu} = \begin{pmatrix} -E G_p B & -E G_p \\ -C G_p B & -C G_p \end{pmatrix},$$

where

$$G_p = (sI - A)^{-1}.$$

$N(s)$ is found by closing the feedback loop for the generalized controller, $u = -Kv$ (negative sign since in the general configuration positive feedback is used), thus

$$\begin{pmatrix} u_c \\ u_f \end{pmatrix} = \begin{pmatrix} -K_c & 0 \\ 0 & -K_f \end{pmatrix} \begin{pmatrix} e_c \\ e_f \end{pmatrix}.$$

6.2 Robust stability tests

The $M\Delta$-structure in figure 3 is used for robust stability analysis. The upper bound of $\mu(M)$ is calculated using the Matlab Robust Control toolbox command `mussv`. Figure 7 shows $\mu(M)$ and $\bar{\sigma}(M)$ for two different levels of uncertainty in the A and B-matrices (10% and 40% in both) at one operating point ($h = 0.7$). The figure shows that the condition $\bar{\sigma}(M) \le 1$ is too conservative when

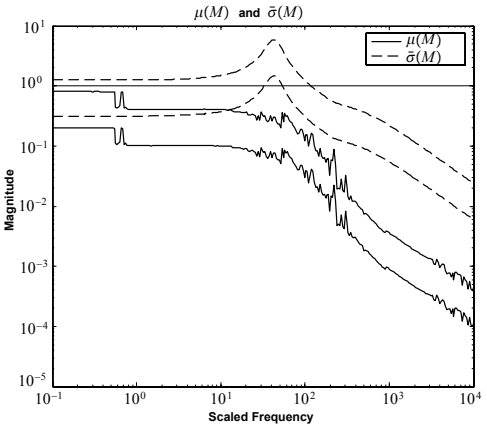

Fig. 7. $\mu(M)$ and $\bar{\sigma}(M)$ for two different levels of uncertainty in the A and B-matrices at one operating point ($h = 0.7$). The condition $\bar{\sigma}(M) \leq 1$ is too conservative when Δ is block-diagonal.

Δ is block-diagonal. According to the robust stability condition in (5), the controller gain should be detuned in order to achieve robust stability for uncertainties larger than 40% at operating point $h = 0.7$. The test for robust stability should be performed at all operating points. There is no guarantee that the tests of the linearized subsystems holds for the total nonlinear system, but such robust stability will give a hint about the robustness properties for the nonlinear system.

7. CONCLUSIONS

The goal of the reported work is to study the robustness properties of a solidification system with a Kalman filter and a gain-scheduled PI-controller. Parametric uncertainty is introduced to the state space model, and by QR-factorization a simple method for pulling out the uncertainty matrix is illustrated. The test cases show that the singular value criteria is too conservative when the uncertainty is represented by a block-diagonal matrix.

In this study, the radiation and conduction dynamics for the control devices at the boundaries have been neglected. Also, in the simulated cases, temperature measurements are assumed to be available in the melt. However, in most practical industrial processes, only temperature measurements outside the mould wall are available. The method proposed in this paper, can be utilized for more realistic instrumentation settings. Then the model should be extended to include state variables of the temperatures outside the mould walls, and more complex boundary conditions must be modeled. The model extensions as well as validation with plant data is ongoing and will be included in future work.

REFERENCES

Batur, C., A. Srinivasan, W.M.B. Duval, N.B. Singh and D. Golovaty (1999). On-line control of solid-liquid interface by state feedback. *Journal of Crystal Growth* **205**, 395–409.

Bonvin, D. (1998). Optimal operation of batch reactors - a personal view. *Journal of Process Control* **8**, 355–368.

Burl, J.B. (1999). *Linear Optimal Control - H2 and Hinfinity Methods*. Addison Wesley Longman, Inc.

Chun, C.K. and S.O. Park (2000). A Fixed-Grid Finite-Difference Method for Phase-Change Problems. *Numerical Heat Transfer, Part B* **38**, 59–73.

Drevermann, A., C. Pickmann, L. Sturz and G. Zimmermann (2004*a*). Observation and control of solidification processes by ultrasonic pulse-echo technique. In: *IEEE International Ultrasonics, Ferroelectrics, and Frequency Control 50th Anniversary Joint Conference*.

Drevermann, A., C. Pickmann, R. Tiefers and G. Zimmermann (2004*b*). Online process control for directional solidification by ultrasonic pulse echo technique. *Ultrasonics* **42**, 105–108.

Friedland, B. (1986). *Control System Design - An Introduction to State-Space Methods*. McGraw-Hill.

Furenes, B. and B. Lie (2006*a*). Solidification and control of a liquid metal column. *Simulation Modelling Practice and Theory* **14 (8)**, 1112–1120.

Furenes, B. and B. Lie (2006*b*). Using event location in finite-difference methods for phase-change problems. *Numerical Heat Transfer, Part B* **50**, 143–155.

Greiss, F.K. and W.H. Ray (1980). Stochastic Control of Processes Having Moving Boundaries - An Experimental Study. *Automatica* **16**, 157–166.

Lewis, F.L. (1986). *Optimal Estimation*. John Wiley and Sons, Inc.

Petersen, I.R. and A.V. Savkin (1999). *Robust Kalman Filtering for Signals and Systems with Large Uncertainties*. Birkhäuser Boston.

Ray, W.H., F.K. Greiss and G.K. Lausterer (1979). Some potential applications of distributed parameter systems theory to metallurgical heating and casting operations. *Metallurgical Transactions B* **10B**, 534–537.

Skogestad, S. and I. Postlethwaite (1996). *Multivariable Feedback Control - Analysis and Design*. John Wiley and Sons.

Weinmann, A. (1991). *Uncertain Models and Robust Control*. Springer.